# Tests of Isospin Mixing Corrections in Superallowed $0^+ \rightarrow 0^+$ $\beta$ Decays

E. Hagberg,[1] V. T. Koslowsky,[1] J. C. Hardy,[1] I. S. Towner,[1] J. G. Hykawy,[1,2] G. Savard,[1] and T. Shinozuka[3]

[1]*AECL Research, Chalk River Laboratories, Chalk River, Ontario, Canada K0J 1J0*

[2]*Physics Department, University of Manitoba, Winnipeg, Manitoba, Canada R3T 2N2*

[3]*Cyclotron and Radioisotope Centre, Tohoku University, Sendai, Japan*

(Received 14 March 1994)

Measurements of superallowed $0^+ \rightarrow 0^+$ nuclear $\beta$ decays, corrected for radiative and charge-dependent effects, yield fundamental properties of the weak interaction. Model predictions of the necessary corrections exist, but they have never been tested directly by experiment. The present work reports, for the first time, observations of (or limits on) nonanalog $0^+ \rightarrow 0^+$ branches in $^{38m}$K, $^{46}$V, $^{50}$Mn, and $^{54}$Co, and tests of the model predictions for isospin-mixing corrections. The resulting unitarity test of the top row of the Kobayashi-Maskawa matrix is $0.9983 \pm 0.0015$.

PACS numbers: 23.40.−s, 12.15.Hh, 24.80.Ba, 27.40.+z

Studies of superallowed nuclear $\beta$ decays between analog $0^+$ states provide data that permit stringent tests of the properties of the electroweak interaction [1–3]. These studies are attractive because, to the extent that isospin is a conserved quantum number, there is a very simple relation between the weak vector coupling constant and the measured $ft$ values for such decays. In reality, some complications arise because bremsstrahlung and related processes need to be accounted for through radiative corrections [2,4,5] and because Coulomb and charge-dependent forces do, in fact, break the isospin symmetry [6–8]. When calculated corrections are included to account for these effects, the corrected $ft$ value, denoted $\mathcal{F}t$, is related to the effective weak vector coupling constant, $G_V'$, as follows (for $T = 1$ states):

$$\mathcal{F}t = ft(1 + \delta_R)(1 - \delta_C) = \frac{K}{2G_V'^2}, \qquad (1)$$

where $f$ is the statistical rate function, $t$ is the partial half-life for the transition, $\delta_R$ is the calculated radiative correction, $\delta_C$ the calculated isospin symmetry-breaking correction, and $K$ is a known constant [1].

Superallowed nuclear $\beta$ transitions are examples of semileptonic weak decay and the value for $G_V'$ obtained from them can, when combined with the value obtained from the purely leptonic muon decay, yield a value for the $V_{ud}$ quark mixing element of the Kobayashi-Maskawa (KM) matrix (see, for example, [1]). Tests of the unitarity of this matrix, for instance,

$$V_{ud}^2 + V_{us}^2 + V_{ub}^2 = 1, \qquad (2)$$

establish limits to extensions of the standard model such as the existence of additional gauge bosons or right-handed currents [2]. Unfortunately, the value for $G_V'$ deduced from an average of the eight most precisely known superallowed $0^+ \rightarrow 0^+$ $\beta$ emitters, $^{14}$O, $^{26m}$Al, $^{34}$Cl, $^{38m}$K, $^{42}$Sc, $^{46}$V, $^{50}$Mn, and $^{54}$Co, disagrees by several standard deviations with the value obtained from the decay of the neutron [9,10].

The $\mathcal{F}t$ and $G_V'$ values deduced from nuclear $\beta$ decays are statistically much more precise than those deduced from the neutron decay. However, there is some room, albeit small, for different interpretations of the $\beta$-decay data. In accordance with the conserved vector current hypothesis, the $\mathcal{F}t$ values for all eight $\beta$-decay cases should be identical; the best overall $\mathcal{F}t$ value should thus be obtained from an average of the eight individual cases [1,2]. An alternative interpretation of the data, however, makes the assumption that there is a residual $Z$ dependence in the $\mathcal{F}t$ values due to processes not accounted for in the usual $\delta_C$ correction; in that case, the best overall $\mathcal{F}t$ value is taken from a curve fitted to the eight individual points and extrapolated to $Z = 0$ [3,11]. With $G_V'$ deduced from $\beta$ decays, the unitarity condition [Eq. (2)] is less than 1 in one-parameter fits, but is met in two-parameter fits; it exceeds 1 if the neutron $G_V'$ value is used.

In order to pursue issues like these, one must examine the two correction terms in Eq. (1). By far, the largest contribution to the $\mathcal{F}t$ value uncertainty comes from the calculations of $\delta_C$ and $\delta_R$, not from the experimental data.

The charge-dependent correction $\delta_C$, in particular, reflects differences between the initial- and final-state wave functions, and thus is strongly nuclear-structure dependent. The two most complete calculations of this correction, which use the Towner-Hardy-Harvey (THH) model [1,6,7] and the Ormand-Brown (OB) model [8], show qualitative agreement in that the large variations in $\delta_C$ from nucleus are similar for both models. However, the models differ in their values for the absolute magnitude of the correction.

Both models identify two separate contributions to the charge-dependent correction. The larger, radial-overlap part, $\delta_{\rm RO}$, arises from the fact that protons are less bound than neutrons, so the (initial) proton wave function imperfectly overlaps the (final) neutron one. The smaller, isospin-mixing part $\delta_{\rm IM}$ results from the different degrees of configuration mixing in the wave functions of members of an isospin multiplet.

This paper describes a series of experiments that yield, for the first time, systematic data to test the $\delta_{IM}$ model predictions. For a $0^+ \rightarrow 0^+$ superallowed $\beta$ decay, the analog initial and final states are both subject to isospin mixing because of the presence of charge-dependent forces. The mixing produces a reduction in the overlap for the analog-state transition that depends on the difference between the mixing in the parent and that in the daughter. The mixing also permits vector $\beta$-decay branches to nonanalog $0^+$ states, processes that are expressly forbidden unless those states contain an admixture of the analog configuration. The magnitude of such nonanalog $0^+ \rightarrow 0^+$ branches thus reflects information on the isospin-mixing correction $\delta_{IM}$. If we denote the (Fermi) matrix element for the ground-state transition as $\langle M_0 \rangle$ and that for the nonanalog transition to an excited $0^+$ state as $\langle M_1 \rangle$, then, for states with $(J^\pi, T) = (0^+, 1)$,

$$\langle M_0 \rangle^2 = 2(1 - \delta_C) \simeq 2(1 - \delta_{IM})(1 - \delta_{RO}), \quad (3)$$

$$\langle M_1 \rangle^2 = 2\delta_{IM}^1(1 - \delta_{RO}), \quad (4)$$

where $\delta_{IM}^1$ is essentially the admixture of the $0^+$ ground state into the excited $0^+$ state. The branching ratio $B_1$ to the latter is

$$B_1 \approx \frac{t_0}{t_1} = \frac{f_1}{f_0}\frac{f_0 t_0}{f_1 t_1} = \frac{f_1}{f_0}\frac{2\delta_{IM}^1}{2(1 - \delta_{IM})} \approx \frac{f_1}{f_0}\delta_{IM}^1, \quad (5)$$

where subscripts 0 and 1 again indicate the ground state and excited $0^+$ state, respectively.

We have searched for nonanalog $0^+ \rightarrow 0^+$ transitions in the decays of four superallowed $\beta$ emitters, viz., $^{38m}$K, $^{46}$V, $^{50}$Mn, and $^{54}$Co. Samples of $^{38m}$K were produced with $(\alpha, n)$ reactions and of the other three activities with $(p, n)$ reactions, all on isotopically enriched targets. The experiments were performed at the TASCC facility, with a helium-jet gas-transfer system used to convey activities from the target chamber to a low-background counting location. There the activity-loaded NaCl aerosol clusters were deposited on an aluminized tape and the collected samples were periodically moved to two detector stations in sequence. The collection time was determined by the removal and insertion of a paddle between the helium-jet nozzle and the tape.

A 68% HPGe detector was used to look for the characteristic $\beta$-delayed $\gamma$ rays from excited $0^+$ states in the daughter. Since the nonanalog transitions are very weak (ppm level) strong samples (MBq level) were required. Passive shielding installed in front of the detector crystal removed direct exposure to the high flux of energetic positrons from the dominant ground-state branch, but the resulting bremsstrahlung radiation was intense enough to obscure any weak $\gamma$-ray branches. To overcome this limitation, we positioned two thin plastic scintillators in front of the HPGe detector and on either side of the transport tape. All recorded $\gamma$ rays were tagged with the status of positron events in the scintillators. If a $\gamma$ ray was observed in coincidence with a positron only in the scintillator on the opposite side of the sample from
it identified an event in which the positron emerged from the sample heading away from the HPGe detector; thus, no bremsstrahlung could have been produced in the shielding. If, however, a positron was observed in each scintillator, it identified an event in which a positron had backscattered in the shielding and then traversed both scintillators; such events were vetoed. When the scintillator conditions were invoked, the level of continuous background in the HPGe spectrum was reduced by a factor of 400 compared to the singles result. This permitted the observation of $\beta$-delayed $\gamma$-ray branches down to the 1 ppm level.

Each sample was assayed in front of the HPGe detector for a few half-lives. The next tape movement brought it into the center of a continuous-flow gas proportional counter where positron events were observed with nearly 100% efficiency and multiscaled. A decay-curve analysis yielded the total number of decays that took place from the activity of interest. Detailed descriptions of the helium-jet system and the counting arrangements have been published elsewhere [9,12].

The results we obtained on the four superallowed $\beta$ emitters are given in Table I. Portions of the corresponding, scintillator-gated $\gamma$-ray spectra are shown in Fig. 1. With our excellent sensitivity to weak transitions, we observed not only nonanalog $0^+ \rightarrow 0^+$ transitions but also the first cases in these emitters of allowed Gamow-Teller (GT) $\beta$ transitions to excited $1^+$ states. The latter transitions are important because they have the effect of altering the accepted branching ratio for the corresponding superallowed branch. Some comments on each of the four cases we studied are given in the following paragraphs. A more detailed description of all new spectroscopic information obtained in our studies will be published in a forthcoming paper [13].

*$^{38m}K$.*—The energy of the first excited $0^+$ state at 3377 keV in $^{38}$Ar and its decay are well known [14]. No evidence for its population from $^{38m}$K $\beta$ decay was observed.

*$^{46}V$.*—Clear evidence of a nonanalog decay branch to the known $0^+$ state in $^{46}$Ti at 2611 keV [15] was found as well as the first observation of a weak (113 ppm) GT transition to a $1^+$ state at 4317 keV. We used both $\gamma$ rays

TABLE I. Summary of experimental data.

| | Samples studied | Number of decays observed | Nonanalog transition $E_\gamma$ (keV) | Peak area | $B_1$ (ppm) |
|---|---|---|---|---|---|
| $^{38m}$K | 63 000 | $5.3 \times 10^9$ | 1210 | <140 | <19 |
| $^{46}$V | 50 000 | $2.6 \times 10^{10}$ | 1722 | 263 | 39(4) |
| $^{50}$Mn | 119 000 | $5.3 \times 10^{10}$ | 3044 | 212 | <3[a] |
| $^{54}$Co | 93 000 | $9.7 \times 10^9$ | 1153 | 763 | 45(6) |

[a]Peak assumed to be a doublet. See text.

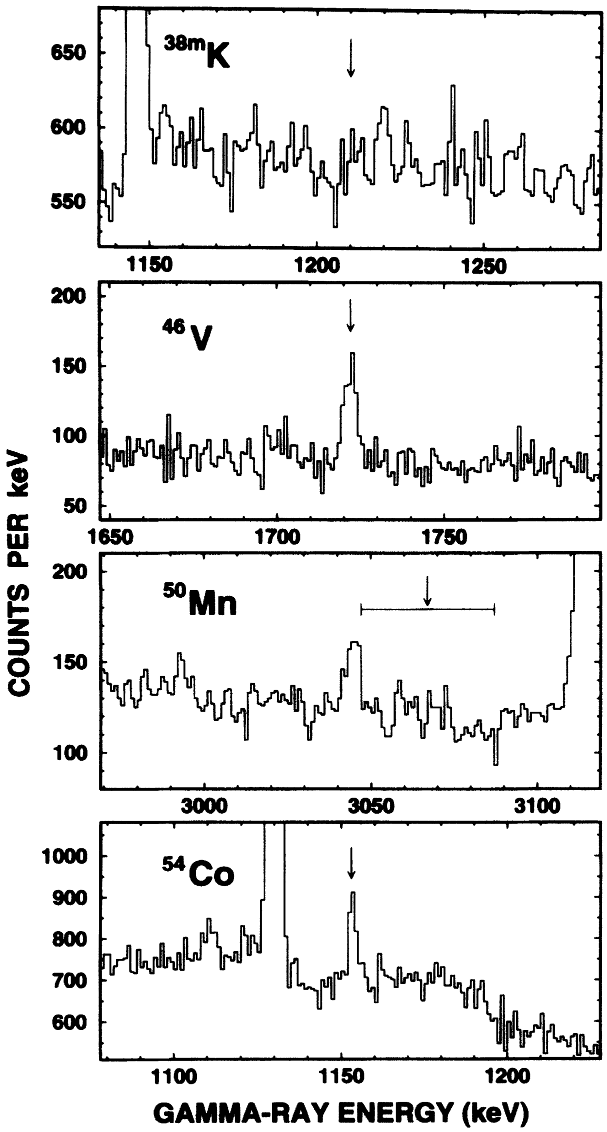


FIG. 1. Portions of gated $\gamma$-ray spectra obtained following the $\beta$ decays of $^{38m}$K, $^{46}$V, $^{50}$Mn, and $^{54}$Co. The position of the expected $0_1^+ \rightarrow 2^+$ $\gamma$ ray is indicated with an arrow in each case. The other big $\gamma$-ray peaks are the double-escape peak of the 2168 keV $\gamma$ ray from the $\beta$ decay of $^{38}$K, the single-escape peak of the 3628 keV $\gamma$ ray from $^{50m}$Mn $\beta$ decay, and the 1130 keV $\gamma$ ray from $^{54m}$Co $\beta$ decay.

from the decay of the $0^+$ state—one at 1722 keV ($0_1^+ \rightarrow 2_1^+$) and the other at 889 keV ($2_1^+, \rightarrow 0^+$)—to evaluate the strength of the nonanalog decay branch, bearing in mind that the GT transition contributes 50% of the intensity of the 889 keV transition.

*$^{50}$Mn.*—Information on excited $0^+$ states in the daughter nucleus, $^{50}$Cr, is very imprecise. There is some evidence for five possible $0^+$ states below 5 MeV excitation [16], but it comes from only a few reaction studies and the excitation energies were not well established. Furthermore, $^{50}$Cr is close to the middle of the *fp* shell so the competing $\beta$ decay of the isomeric state in $^{50}$Mn has many branches, which give rise to many polluting $\gamma$-ray transitions.

We made detailed studies of samples containing a mixture of $^{50}$Mn and $^{50m}$Mn as well as samples containing only the longer-lived $^{50m}$Mn. Several new $\beta$-decay branches and $\gamma$-ray transitions were assigned to the decay of the isomeric state, among them a 3045 keV $\gamma$ ray. With these decays accounted for, we assign two new GT branches to the decay of $^{50}$Mn. They populate $1^+$ states at excitation energies of 3628 and 4998 keV, with branching ratios of 570 and 6.8 ppm, respectively. We found only one other $\gamma$-ray transition that could possibly originate from the $\beta$ decay of $^{50}$Mn. Its energy is 3044 keV and it could therefore be the $\gamma$ ray connecting the second known $0^+$ state in $^{50}$Cr (3850 $\pm$ 20 keV) to the 783 keV $2^+$ state but, as mentioned above, a $\gamma$ ray of similar energy was assigned to the decay of $^{50m}$Mn. The energy of the $\gamma$ ray in the mixed spectrum is distinctly lower than its counterpart in the pure $^{50m}$Mn spectrum, its intensity is greater when normalized to other $\gamma$ rays from $^{50m}$Mn, and it has a shorter decay time. These three observations, all just at or outside the $1\sigma$ level, are consistent with the peak at 3044 keV being a doublet, with one component arising from the decay of $^{50}$Mn and the other one from $^{50m}$Mn. We have therefore concluded that up to 60% of the 3044 keV $\gamma$-ray peak area in the mixed samples run can be due to a nonanalog decay branch of $^{50}$Mn, and we treated this as an upper limit to the strength of that branch.

*$^{54}$Co.*—Clear evidence for a nonanalog decay branch to the known $0^+$ state at 2561 keV in $^{54}$Fe [17] was seen. No GT transitions were observed.

Table II shows the $\delta_{\rm IM}^1$ values derived with Eq. (5) from the experimental nonanalog branches listed in Table I. The values that we have calculated for $\delta_{\rm IM}^1$ using the THH model [7] are shown for comparison; also listed are the $\delta_{\rm IM}$ values (effectively upper limits on $\delta_{\rm IM}^1$) calculated for both the THH and OB [8] model. In general, the THH model $\delta_{\rm IM}^1$ values are in reasonable agreement with the experimental values and in all cases $\delta_{\rm IM}^1$(expt.) $<$ $\delta_{\rm IM}$(theory); i.e., the amount of the analog state found by experiment mixed into an excited $0^+$ state is less than the amount of the calculations claim is mixed out of the ground state. For the OB model, this is not found to be the case. The calculations of both models for the $^{38m}$K, *sd*-shell case, are not severely tested by our data but, for the *fp*-shell cases of $^{46}$V and $^{54}$Co, the OB model results consistently underpredict the extent of isospin mixing. Because the two models are based on very similar concepts, the differences in their predictions probably arise as a result of a too severe truncation of the shell-model space used for the *fp* shell and failure to obtain the correct excitation energy for the first excited $0^+$ state by the OB-model calculations [18].

TABLE II. Isospin mixing corrections.

| Nuclide | Expt. (%) $\delta_{\rm IM}^1$ | Theory (%) THH $\delta_{\rm IM}^1$ | THH $\delta_{\rm IM}$ | OB $\delta_{\rm IM}$ |
|---|---|---|---|---|
| $^{38m}$K | <0.28 | 0.096(2) | 0.100(2) | 0.11 |
| $^{46}$V | 0.053(5) | 0.046(5) | 0.087(10) | 0.01 |
| $^{50}$Mn | <0.016 | 0.051(23) | 0.068(30) | 0.004 |
| $^{54}$Co | 0.035(5) | 0.037(8) | 0.045(5) | 0.005 |

The more significant difference between the THH and OB model predictions, however, occurs for the radial overlap correction $\delta_{\rm RO}$. The new data obtained in the present work do not shed any light on that difference and averages of the two model calculations are therefore used here. However, for the isospin mixing corrections $\delta_{\rm IM}$ in the $fp$ shell, the results from the THH model are now preferred and the use of calculated values for $\delta_{\rm IM}$, in this shell, from this model alone result in a slight increase in the value of $G_V'$. More important, we have provided a sound basis for trusting the calculations of $\delta_{\rm IM}$.

The present work includes the first observation of three allowed GT transitions seen in competition with ground-state superallowed $0^+ \rightarrow 0^+$ $\beta$-decay branches. One of these transitions, in $^{50}$Mn, was intense enough that the $ft$ value for the superallowed branch has been changed significantly. Furthermore, the upper limits established for possible GT branches in the decays of $^{38m}$K and $^{54}$Co are now far below the level at which they could affect the strength of the superallowed branch. Incorporating these results into the world data for $0^+ \rightarrow 0^+$ superallowed decays [1] we obtain $G_V'/(\hbar c)^3 = 1.149\,44(62) \times 10^{-5}\ {\rm GeV}^{-2}$, with the unitarity sum [Eq. (5)] being 0.9965(15).

In summary, a sensitive detection system has permitted us to observe (or set sensitive limits on) nonanalog $0^+ \rightarrow 0^+$ $\beta$ transitions in the decays of four superallowed $\beta$ emitters. The branching-ratio data shown in Table I permit direct tests of charge-dependent mixing models which indicate that the Towner-Hardy-Harvey model is in reasonable agreement with the experimental data for superallowed $\beta$ emitters in the $fp$ shell. With the effects of isospin mixing now established, another source of uncertainty has been removed form nuclear measurements of the weak vector coupling constant.

The present work also constitutes the first serious search for Gamow-Teller branches in the decays of the superallowed $\beta$ emitters $^{38m}$K, $^{46}$V, $^{50}$Mn, and $^{54}$Co. All cases were probed at least to the level of 50 ppm in branching-ratio level and three GT transitions were found.


[1] J.C. Hardy *et al.*, Nucl. Phys. **A509**, 429 (1990).
[2] I.S. Towner, Nucl. Phys. **A540**, 478 (1992).
[3] P. Quin, Nucl. Phys. **A553**, 319c (1993).
[4] W.J. Marciano and A. Sirlin, Phys. Rev. Lett. **56**, 22 (1986).
[5] W. Jaus and G. Rasche, Phys. Rev. D **41**, 166 (1990).
[6] I.S. Towner, J.C. Hardy, and M. Harvey, Nucl. Phys. **A284**, 269 (1977).
[7] A new calculation is presented here following the strategy discussed by I.S. Towner, in *Symmetry Violations in Subatomic Physics*, edited by B. Castel and P.J. O'Donnel (World Scientific, Singapore, 1989), p. 211.
[8] W.E. Ormand and B.A. Brown, Phys. Rev. Lett. **62**, 866 (1989).
[9] E. Hagberg *et al.*, in *Proceedings of the 6th International Conference on Nuclei far from Stability, Bernkastel-Kues, Germany, 19–24 July 1992*, IOP Conf. Proc. No. 132 (Institute of Physics and Physical Society, London, 1992), p. 783.
[10] H. Ibele and D. Dubbers, in *Proceedings of the 6th International Conference on Nuclei far form Stability* (Ref. [8]).
[11] D.H. Wilkinson, Nucl. Phys. **A511**, 301 (1990).
[12] E. Hagberg *et al.*, Nucl. Phys. A (to be published).
[13] E. Hagberg *et al.* (to be published).
[14] P.M. Endt, Nucl. Phys. **A521**, 1 (1990).
[15] D.E. Alburger, Nucl. Data Sheets **49**, 237 (1986).
[16] T.W. Burrows, Nucl. Data Sheets **61**, 1 (1990).
[17] Hou Junde *et al.*, Nucl. Data Sheets **68**, 887 (1993).
[18] W.E. Ormand (private communication).